Trace gases and CO_2 isotope records from Cabo de Rama, India

S. K. Bhattacharya[1], D. V. Borole[2], R. J. Francey[3], C. E. Allison[3], L. P. Steele[3], P. Krummel[3], R. Langenfelds[3], K. A. Masarie[4], Y. K. Tiwari[5] and P. K. Patra[6,*]

[1]Physical Research Laboratory, Ahmedabad 380 009, India
[2]National Institute of Oceanography, Goa 403 004, India
[3]CSIRO Atmospheric and Marine Research, Aspendale, Victoria 3195, Australia
[4]NOAA Earth System Research Laboratory, Boulder, Colorado 80303, USA
[5]Indian Institute of Tropical Meteorology, Pune 411 008, India
[6]Frontier Research Center for Global Change, JAMSTEC, Yokohama 2360001, Japan

Concentrations of carbon dioxide (CO_2), methane (CH_4), carbon monoxide (CO), nitrous oxide (N_2O) and hydrogen (H_2), and the stable carbon ($\delta^{13}C$–CO_2) and oxygen ($\delta^{18}O$–CO_2) isotopic composition of CO_2 have been measured in air samples collected from Cabo de Rama (CRI), India, for the period 1993–2002. The observations show clear signatures of Northern and Southern Hemispheric (NH and SH) air masses, mixed with their regional fluxes and chemical loss mechanisms, resulting in complex seasonal variation of these gases. The CRI measurements are compared with remote marine sites at Seychelles and Mauna Loa. Simulations of two major anthropogenic greenhouse gases (CO_2 and CH_4) concentrations using a chemistry-transport model for the CRI site suggest that globally optimized fluxes can produce results comparable to the observations. We discuss that CRI observations have provided critical guidance in optimizing the fluxes to constrain the regional source/sinks balance.

Keywords: Cabo de Rama, CO_2 isotope, greenhouse gases, trace gases.

THE greenhouse gases (GHGs) trap earth's outgoing longwave radiation (OLR) and contribute towards increasing the surface temperature. For example, carbon dioxide (CO_2), nitrous oxide (N_2O) and methane (CH_4) jointly constitute 70% of all the positive radiative forcing (RF) in 2005 of 3.28 Wm^{-2}, and 143% of the net RF of 1.6 Wm^{-2}, as estimated by the Intergovernmental Panel on Climate Change[1]. The share of these three major GHGs is likely to be more significant in the future because some of the other gases, such as halocarbons and tropospheric O_3, are either being controlled effectively under mitigation strategies or have shorter atmospheric lifetimes. Lifetimes of CO_2, N_2O and CH_4 are ~100, 120 and 8.4 years in the atmosphere respectively[2]. Longer lifetimes also slow down the response of emission reduction agreements, thus reinforcing the need for early action to avoid dangerous climate change due to GHG forced warming. Concentrations of CO_2, CH_4 and N_2O have increased at alarming rates, from preindustrial values of 280 ppm, 715 ppb and 270 ppb (circa. 1750) to 379 ppm, 1732 ppb and 319 ppb respectively in 2005 (ref. 1).

With the implementation of the Kyoto protocol and associated carbon trading coming into effect, the demand for high-quality measurements of these gases in the troposphere, covering local/regional and long-time scales is increasing. While the global average increase of these long-lived GHGs is important for RF calculations, monitoring at a large number of sites is required for estimating sources/sinks at sub-continental or country scales. Generally, such measurements from the developing part of the world (Asia except Japan or South Korea, Africa, and South America) are sparse even today[3,4]. To the best of our knowledge, no long-term monitoring site where measurements are made at regular intervals exists in India. Measurements of GHGs (mainly CH_4) have mostly been made on a campaign basis or with large data gaps, making them unsuitable for systematic analysis of decadal trends and variability[5,6].

In the early 1990s, a GHG measurement site was established at Cabo de Rama, India, as a collaborative effort of CSIRO Marine and Atmospheric Research (CMAR), Physical Research Laboratory (PRL), and National Institute of Oceanography (NIO). Apart from the fact that CRI is located in a data sparse region, the large-scale atmospheric circulation over the Indian Ocean/Arabian Sea and the Indian subcontinent, which is characterized by biannual reversal in low-level winds associated with the Indian monsoons[7], makes this site quite interesting for testing the capabilities of state-of-the-art chemistry-transport models (CTMs) in simulating the meteorology and trace gas concentrations. Here we describe the CRI location characteristics, time series of several trace gases and isotopic composition of CO_2, and compare the GHG observations with CTM simulations to discuss the role of measurements from this site in constraining regional sources/sinks. Measurements from this site are also put in a global perspective by comparison with the nearest long-term monitoring sites at Seychelles (SEY), Mahe Island (Indian Ocean) and Mauna Loa (MLO), Hawaii (Pacific Ocean).

After some preliminary site exploration, Cabo de Rama on the West Coast of India (marked 'C' in Figure 1) about 80 km south of Panaji, Goa (73.9°E, 15.1°N) was selected. The sampling location is on a flat rocky terrain, about 60 m above sea level. The site is devoid of vegetation over a scale of 50 m on all sides and is at least a few hundred metres away from sparse habitation. The meteorological data from Panaji show that in this part of the west coast, the wind in the afternoon (sampling time) is from the sea (onshore) all year round. In the northern

*For correspondence. (e-mail: prabir@jamstec.go.jp)

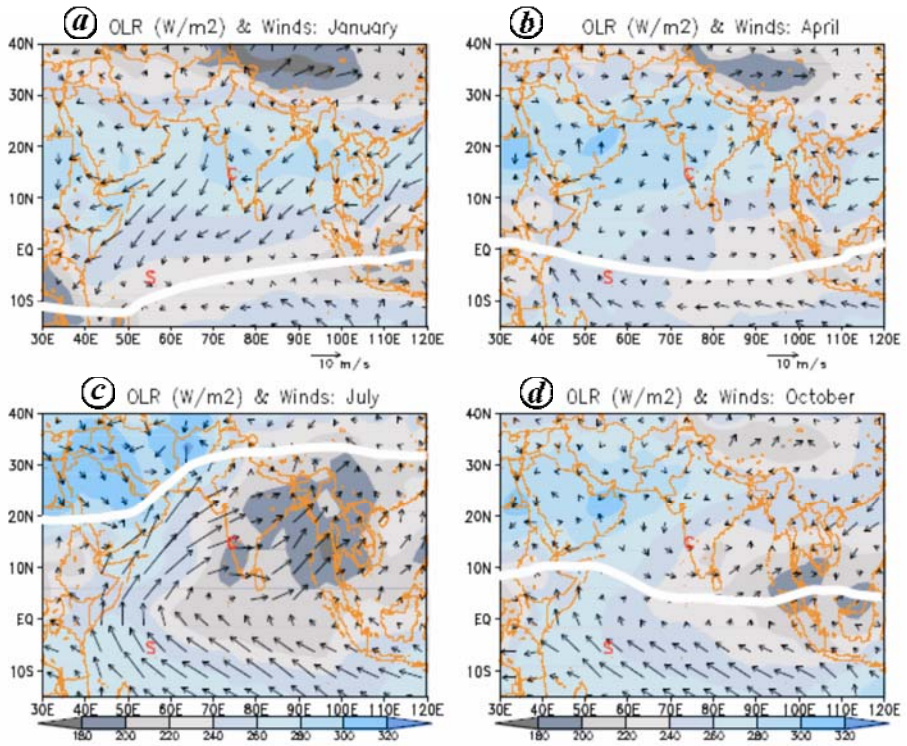

Figure 1. Locations of the CRI and SEY air sampling sites, marked as 'C' and 'S' in red. The general direction of wind flow during the SW monsoon is from SEY to CRI in July and opposite during the NE monsoon season (January). The location of the ITCZ, defined as the lowest wind intensity and a meeting point of north–south winds, is marked by a white line in each panel.

summer (SW) monsoon period, this flow direction matches with the general large-scale flow and CRI is located south of the inter-tropical convergence zone (ITCZ) as shown in Figure 1. Therefore, air samples collected during this period (June to September) represent tropical or SH oceanic air mass, representative of a wider area, and not contaminated by large industrial emission or strong ecosystem exchanges. In the northern winter (NE) monsoon period, the zonal wind direction is from the land to the sea and matches with the morning local wind (offshore). However, the same air mass is recirculated by afternoon sea breezes[8], with some dilution of continental trace gas signatures.

The wind speed at the time of sampling was moderate, generally about 4–6 m/s but increasing to 10–12 m/s at the peak of the SW monsoon. All India average rainfall varied from near zero to about 250 mm month^{-1}, which is the primary resource for agricultural activity[9] and terrestrial ecosystem productivity in most parts of the Indian subcontinent. It is therefore expected that the two monsoon systems must have an important effect on the concentration and isotopic composition of atmospheric CO_2, and the concentrations of other trace gases. Air sampling at CRI contributes to the global atmospheric composition study[10,11]. Given the potential for global impacts originating in the poorly sampled tropical/sub-tropical regions, data from this site provide valuable constraints on global/regional GHG forcing. During the roughly 10 years of regular sampling, CRI was one of the most influential sites in constraining large-scale source and sinks of CO_2. This arose from its proximity to a large region subject to large uncertainties and otherwise poorly sampled. For example, Rayner *et al.*[12] showed the importance of the CRI $\delta^{13}C$–CO_2 record in constraining fluxes from the adjacent land region.

Chemically dried (using anhydrous $Mg(ClO_4)_2$) air samples are collected in 500 ml glass flasks at a pressure of 1900 hPa (absolute) using a specially designed portable flask pump unit equipped with digital wind speed and wind direction monitors. The air-intake is 6 m above ground and two flasks are pressurized, one after another, during each visit to the site. Each flask is flushed at around 4 litre min^{-1} with (dried) air for about 10 min before filling. After filling, the flasks are returned to CMAR's GASLAB (Global Atmospheric Sampling LABoratory) in Aspendale for determination of the concentrations of trace gases CO_2, CH_4, CO, N_2O and H_2 by gas-chromatographic methods with measurement precision of 0.07 ppm, 2.4 ppb, 1.0 ppb, 0.3 ppb, 1.0 ppb respectively[13]. Subsequently, the carbon and oxygen isotopic ratios in CO_2 are determined using an automatic cryogenic extraction system coupled to a Finnigan Mat 252 mass-spectrometer with internal precision of 0.015‰ and 0.04‰ for $\delta^{13}C$–CO_2 and $\delta^{18}O$–CO_2 measurements

respectively. Further details of GASLAB operation are given in Francey *et al.*[10,14] and extensive detail of uncertainty in isotope measurements is given in Allison and Francey[15]. Based on the intercomparison programme (ICP) at Cape Grim, CO absolute scale at CMAR is about 2 to 4 ppb higher compared to the ESRL scale, and that for H_2 are in the range of –10 to 20 ppb and –4 to 6 ppb in the period of 1992–96 and 1997–2002 respectively.

Data are routinely corrected for drift in CO_2 mixing ratio associated with storage of air samples in glass flasks fitted with polymer O-rings. Such drift is primarily due to permeation of gases through the O-rings[16]. Corrections are dependent on the duration of storage and the flask type (volume, number and material of O-rings), and are based on both empirical results of laboratory storage tests[17] and observed discontinuities in CO_2 time series observed at high-latitude southern hemisphere sampling sites (Macquarie Island, Casey, Mawson and South Pole), where deviations are tightly correlated with storage time. Between 1993 and 2001, most samples were analysed within 12 months of collection, with a mean storage time of 6 months. The final batch of samples received at CSIRO contained air collected between May 2001 and October 2002. They were not analysed until June/July 2003 so that storage times for these samples were up to 25 months.

We have used the Centre for Climate System Research/ National Institute for Environmental Studies/Frontier Research Centre for Global Change (CCSR/NIES/FRCGC) atmospheric general circulation model (AGCM) based CTM (hereafter, ACTM[18]) for simulating the GHGs in the altitude range of earth's surface to the mesosphere (~90 km). The forward simulation results for CO_2 using ACTM and two other models have been compared with observations at CRI and are discussed separately[19]. Detailed analysis of CH_4 at many sites globally (including CRI) and at hourly-decadal timescales is also available in the literature[20]. The model horizontal resolution is set at T42 spectral truncations (~$2.8 \times 2.8°$) and 67 pressure-sigma layers in the vertical. Due to the coarse horizontal resolution of ACTM, the model simulations are expected to capture regionally representative features in long-lived trace gases arising from flux distributions and meteorology. Thus, potential bias caused by land–sea breeze conditions cannot be addressed with this model due to the coarse horizontal resolution.

In February 1993, regular flask sampling was started at CRI, where duplicate flask samples have been collected twice every month till 2002. The measurement records for the whole sampling period are presented here in the form of time series plots (Figures 2 and 3). Data have been submitted to the WDCGG and CDIAC international databases. For each species, we produced a smooth fit to the data by applying a Butterworth digital filtering routine to convert data into the frequency domain, applying a low-pass filter and then applying an inverse FFT to get back to the time domain. The filter[21] effectively removes variations with periods less than 22 days. Smooth fitted data from Cabo de Rama (15.1°N, 73.8°E) are compared to smoothed CMAR data from Mauna Loa (19.5°N, 155.6°W) representing zonal-mean NH marine-air mass, and smoothed NOAA Earth System Research Laboratory (ESRL) measurements from Seychelles (4.7°S, 55.2°E) which is located upwind of CRI during the SW monsoon, and down-wind of the Indian subcontinent during the NE monsoon. Comparisons with SEY are presented for those species (CO_2 and its isotopes and CH_4) where ESRL and CMAR data are reported on the same scales, and inter-laboratory differences have been demonstrated to be generally insignificant for our data analysis by ongoing sample measurement intercomparisons using flask air from Cape Grim[13,22].

In Figure 2, the CRI CO_2 mixing ratio (symbols and the fitted black line) is compared to a smooth curve fitted to CSIRO MLO data (blue line) and to the SEY data (red line). MLO seasonality is predominantly influenced by the large carbon uptake–release cycle of the terrestrial ecosystem in the NH mid- and high-latitudes, whereas SEY, within the ITCZ, is a mixture of NH and SH air with mean value closer to SH values and exhibits complex, perhaps competing seasonality. At CRI the large seasonality is more determined by large scale transport that introduces SH air or NH air in different seasons. We note that CRI data density is sometimes too sparse to precisely determine seasonal amplitude, and that data quality is less reliable in the first 1–2 years of establishment. Note also that the time of flask sampling was varied between 10 : 00 and 13 : 00 local time (LT, or Indian Standard Time, IST), and was delayed by about two hours to 12 : 30–13 : 30 LT for the period after 1997. Although the influence of this change is not visible in significant changes relative to SEY, a clearer assessment awaits improved information on the diurnal cycle for different wind regimes.

At CRI, the highest CO_2 mixing ratio is observed in February–March, towards the end of the NE monsoon when the vegetation activity in northern India is dominated by heterotrophic respiration and anthropogenic emissions are high. The seasonal minimum in mixing ratio occurs in October, soon after the SW monsoon, when the local vegetation activity is still dominantly photosynthetic. The effect of maximum photosynthetic uptake during July–August is not recorded at this site because the winds are strong and south-westerly (representative of the SH air mass). This situation complicates the interpretation of seasonal cycle amplitude at CRI compared to that expected at other sites. During the SW monsoon, CO_2 concentrations observed at CRI agree well with those observed at SEY. Because of the strong prevailing wind speed during the SW monsoon, possibility of large influence due to upwelling in the Arabian Sea at this time is unlikely to be recorded at CRI. The eastern and central Arabian Sea acts as a weak to strong source of CO_2, up to

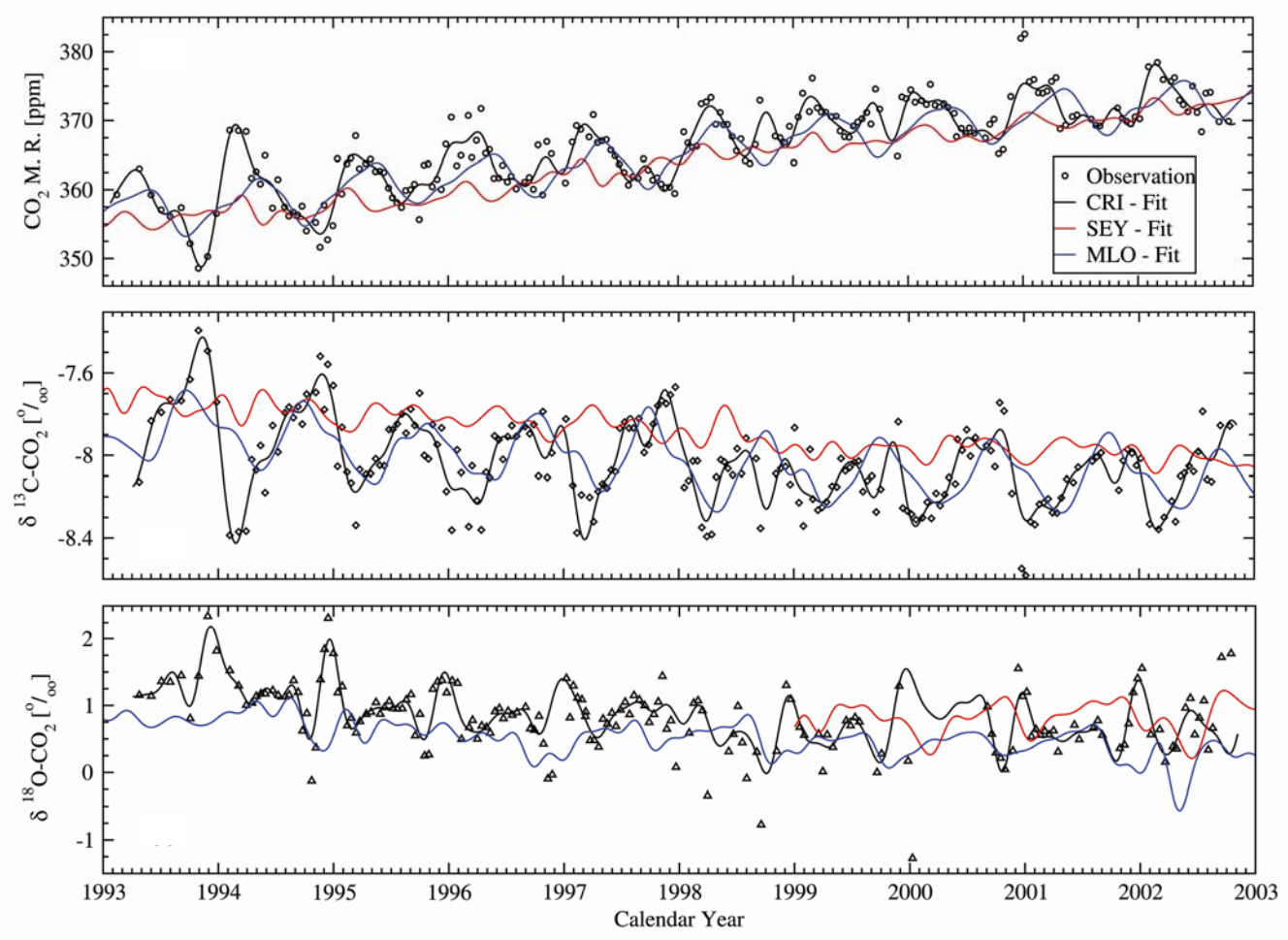

Figure 2. Measured concentrations of CO_2 (top), $\delta^{13}C$–CO_2 (middle), $\delta^{18}O$–CO_2 (bottom) in air samples collected at CRI (symbol) along with fitted curve to the data points using a digital filter (black line). Smoothed fits to the Mauna Loa (blue line) and SEY data (red line) obtained by CSIRO and ESRL programs respectively, are shown for comparison. The $\delta^{18}O$–CO_2 data prior to 1999 at SEY are excluded due to sampling error specific to this species. At CRI, more than 50% of the 120 samples collected from start-1998 to start-2001 had $\delta^{18}O$–CO_2 values less than zero. Most negative values were rejected after a statistical filter (3σ) but quite a few remained, and are excluded by the digital filter while preparing the fitted line (black).

about 1.7 g CO_2 m^{-2} day^{-1} during the SW monsoon[23], but is much weaker than the flux variability estimated over the land ($\pm$ 10 g CO_2 m^{-2} day^{-1}).

Until October–November, CRI CO_2 absolute concentrations are generally close to those at SEY. From autumn to spring, CRI values increase sharply to values much higher than at SEY. These elevated CO_2 levels are consistent with contemporary variations observed generally in the NH, as represented here by the MLO record though there are clear differences in the phase of the average seasonal cycles. The CRI and SEY differences are also consistent with regional net (photosynthetic) uptake in October–November, followed by net winter respiration.

The negative correlation between the CRI $\delta^{13}C$–CO_2 (Figure 2 *b*; see also ref. 13) and CO_2 mixing ratio on the seasonal timescale favours a strong biogenic contribution, and excludes a strong oceanic contribution. The coefficients for each year from 1993 to 1998 are –0.0433, –0.0478, –0.0476, –0.0467, –0.0551 and –0.0408‰ ppm^{-1} respectively. While the differences in the coefficients are of marginal significance, it is suggestive that the largest values occur in 1994 and 1997, the years of enhanced biomass burning, and the lowest values occur in the immediately following years. Such a pattern would be expected if a higher proportion of C_3 photosynthetic material were involved in global exchange in 1994 and, particularly in 1997, followed by an increased C_4 proportion in the subsequent year. This pattern is expected if wild fires convert tropical forest to Savannah, or involve persistent combustion of peat as occurred in the 1997 Indonesian fires[24,25]. Further analysis is required to attribute exact causes for the year-to-year variability in stable isotopes of CO_2.

The $\delta^{18}O$-CO_2 values (Figure 2 *c*) exhibit a complex seasonal behaviour, with relatively steady values, close to SH values observed at other GASLAB sites, during the SW monsoon. A small decrease in $\delta^{18}O$–CO_2 is observed at the end of the SW monsoon and is followed by a rapid

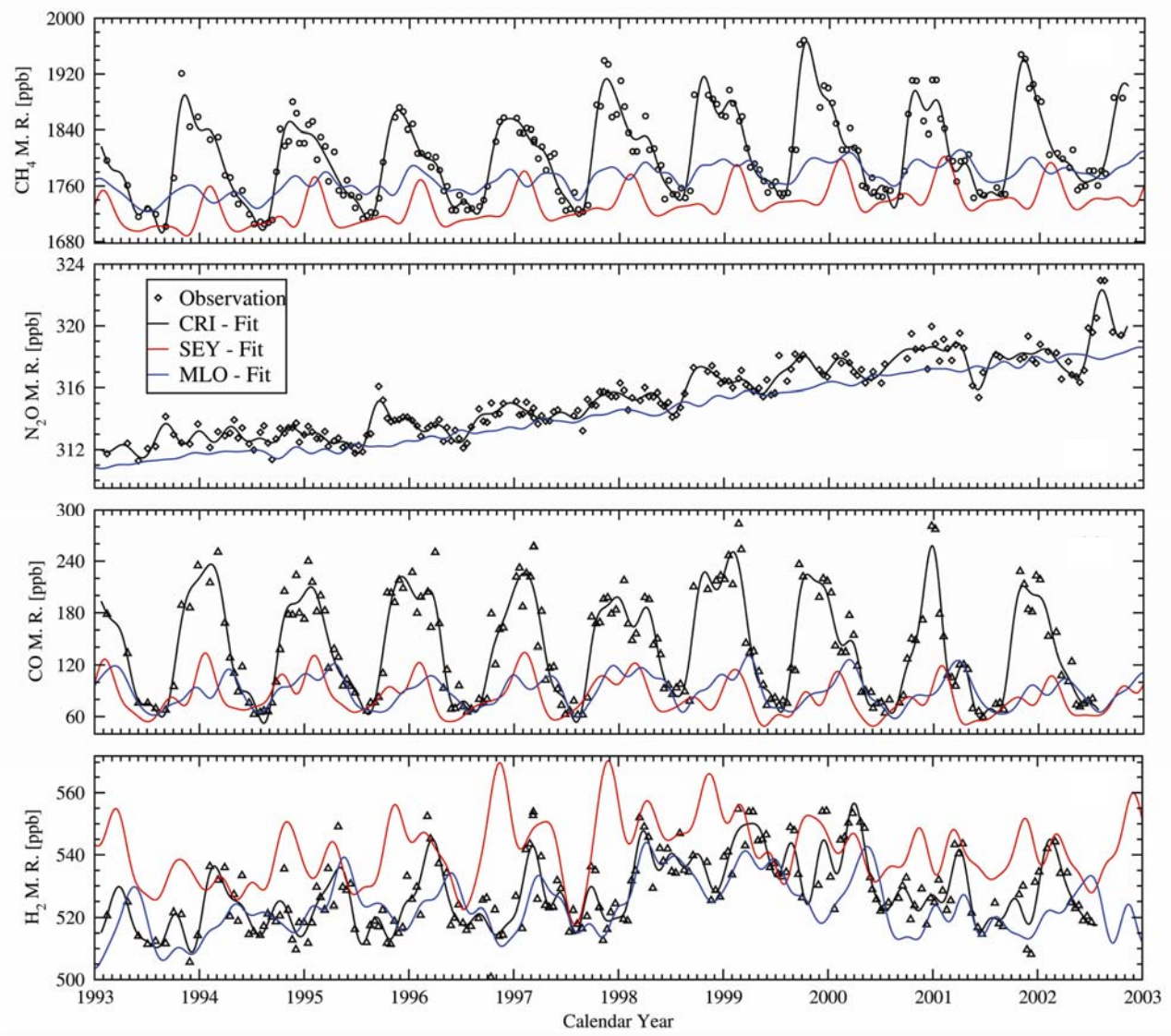

Figure 3. Same as Figure 2, but for CH_4, N_2O, CO and H_2. Smoothed fits to the Mauna Loa (blue line; data source: CMAR) or SEY data (red line; except for N_2O; data source: ESRL) are given for comparison.

increase to a high value at the beginning of the NE monsoon. Data quality seriously deteriorates between 1998 and 2001 due to anomalies with drying or flask storage. The $\delta^{18}O$–CO_2 values in the SW monsoon period show a general decline of around 0.5‰ from 1993 to 1996, followed by a flattening that has been observed elsewhere in the CSIRO global network. The more positive peak in $\delta^{18}O$–CO_2 in the NE monsoon period compared to the SW monsoon period is opposite to that expected from large scale interhemispheric gradients that show MLO values around 1 per mille more negative than mid- to high-latitude SH values[26]. The reverse gradient is most easily explained by an isotopic exchange with leaf water, which is significantly enriched compared to soil water, particularly in conditions of high evapotranspiration.

Variations in mixing ratios of CH_4, N_2O, CO and H_2 at CRI are shown in Figure 3, along with smooth curves fitted to the MLO (and CH_4 only at SEY) data. As expected, the CRI and SEY values are quite similar for CH_4 during the SW monsoon period for all years, but the CRI data are significantly elevated during the NE monsoon period. Over the whole year, seasonal cycle phases for CH_4 and CO at CRI are quite similar (correlation coefficient = 0.87), which might be expected if changes in monsoon meteorology expose strong emission of both these gases due to anthropogenic activity in India. This is unlike the dominating role of terrestrial ecosystem activity in controlling the CO_2 seasonal cycle at CRI. The seasonal minimum during the summer time in most parts of the world is produced by loss of these gases due to chemical reaction with OH[20]. The mixing ratios start to increase strongly just after the SW monsoon when the origin of the air mass changes to NW or NNW direction, carrying mainly continental air. CH_4 peaks at the beginning of the

NE monsoon and then steadily decreases through to the beginning of the next SW monsoon. The highest CO values are obtained throughout the NE monsoon, reflecting high emissions from the Indian subcontinent. General features of the constituents transport during the NE monsoon season have been established during the Indian Ocean Experiment (INDOEX)[27].

The post SW monsoon increase in CH_4 is also clear in the SEY data but occurs later, in early December (i.e. during the developed phase of the NE monsoon in India), when the continental air starts to arrive at SEY. At this time, the ITCZ position coincides with the SEY latitude (4°S) and the winter continental air starts to flow over it (Figure 1 *b*). Subsequently, during the northward migration of the ITCZ as it moves past SEY, the supply of continental air is cut off and the equatorial marine value is returned there. On the contrary, CRI continues to have higher mixing ratios until June as it still continues to receive continental air. The net result of this is that the peaks in CH_4 at SEY are flanked on both sides by the peaks at CRI, and the peak value observed at SEY is smaller compared to that at CRI due to dilution of the continental emission signal by the marine air. It is interesting to note here that the CH_4 mixing ratios at MLO are higher compared to CRI during the SW monsoon season (June–August). This gives evidence that the exchange of air between the hemispheres is more efficient in the Indian Ocean sector than the Pacific Ocean sector.

The N_2O mixing ratio (Figure 3 *b*) does not show a well organized seasonal cycle at the available measurement precision. The smaller seasonal cycle amplitude is due to small seasonality in fluxes and no measurable loss of N_2O in the troposphere (unlike CO and CH_4). Thus, the horizontal and vertical gradients in N_2O mixing ratio are likely to be small in the troposphere; e.g. the difference between Cape Grim and Mace Head is found to be about 3 ppb or less[28]. Thus the change in monsoon meteorology cannot introduce a large change in N_2O mixing ratio with seasons at this site. From 1993 to mid-1995, the mean value remained close to 313 ppb, but increased steadily after that reaching 320 ppb in 2002. The baseline N_2O mixing ratios (defined as the seasonal minimum) at MLO and CRI are within 1 ppb of each other, but about 2–3 ppb higher at CRI than that at MLO in the NE monsoon season, indicating that the regional emission in the vicinity of the CRI site is higher than the global average (including both the ocean and land regions) emission. As stated earlier, the MLO site is fairly representative of the NH mean mixing ratio for the long-lived gases. The importance of CRI timeseries in constraining south Asian N_2O emission has been discussed recently[29].

In comparison, H_2 is consumed rapidly by the land surface and by reacting with OH. Thus, the SEY site mostly shows higher mixing ratio compared to CRI or MLO sites (Figure 3 *d*). Again, the SEY and CRI values are in good agreement in the SW monsoon season, but H_2 mixing ratios increase sharply at SEY in the post-monsoon season (September–December) when the ITCZ is located in between and separating these two sites by about equal distance (Figure 1 *c*). In the NE monsoon period, the mixing ratios at CRI and SEY are similar.

Figure 4 shows the model-observation comparisons of CH_4. The model results are given as the daily average mixing ratios as sampled at CRI and the fitted curves refer to both the model and observations. The assumption remains that during sampling in sea-breeze conditions trace gas levels reflect integrated emissions from the continent, except during the SW monsoon season. Details of CH_4 model-observation comparison at this site in relation to monsoon dynamics and SEY observations have been discussed recently[20], and only a brief account is given here. Comparison with MLO (Figure 3 *a*) suggested stronger emissions from the Indian subcontinent, and the comparison with model results as shown here (Figure 4) is based on an estimate that annual total emission from India would be about 41 Tg–CH_4 yr^{-1} (ref. 20). This emission estimate is obtained by model-observation comparison of CH_4 time series at CRI. The phase of the average seasonal cycle and synoptic scale variability at CRI and SEY are well reproduced by the ACTM simulation. Such agreement in model-observation time series is attributed to the realistic representation of model transport in the troposphere and stratosphere–troposphere exchange (STE), loss of CH_4 by reacting with OH and surface fluxes[20]. These model-observation comparisons illustrate the causes for trace gas variations at seasonal scale and support the proposition made in Lal *et al.*[5] using dual tracer analysis (SF_6 and CH_4) at Tiruvananthapuram, a site located in the southernmost point of India. Unfortunately, operation of that site is also discontinued.

Figure 5 shows interannual (IAV; right column) and interseasonal variability (ISV; left column) in all the gases and CO_2 isotopic compositions at CRI. The IAVs and ISVs are defined as time-derivative of the long-term trends component and the fitted curve respectively, for each timeseries at daily intervals obtained by digital filtering. Only the CH_4 simulation results are compared with observations here (see ref. 19, for model-observation comparison of CO_2). The combination of ISV and IAV analysis helps us to understand the rise and fall timing of the seasonal variations and interannual variations respectively. From the ISV time series, we can clearly see that the CO_2 mixing ratio rises rapidly during the autumn season around this site, the decrease in $\delta^{13}C$–CO_2 suggesting an increase in anthropogenic (fossil fuel and biomass burning) or respiration components contribution to atmospheric CO_2. This one-to-one negative correlation is also valid for the IAV of CO_2 and $\delta^{13}C$–CO_2. Large positive (negative) IAVs in CO_2 ($\delta^{13}C$–CO_2) are shown to result from dry tropical conditions during the El Niño periods of 1992–1994 and 1997/98 (refs 12, 24 and 30).

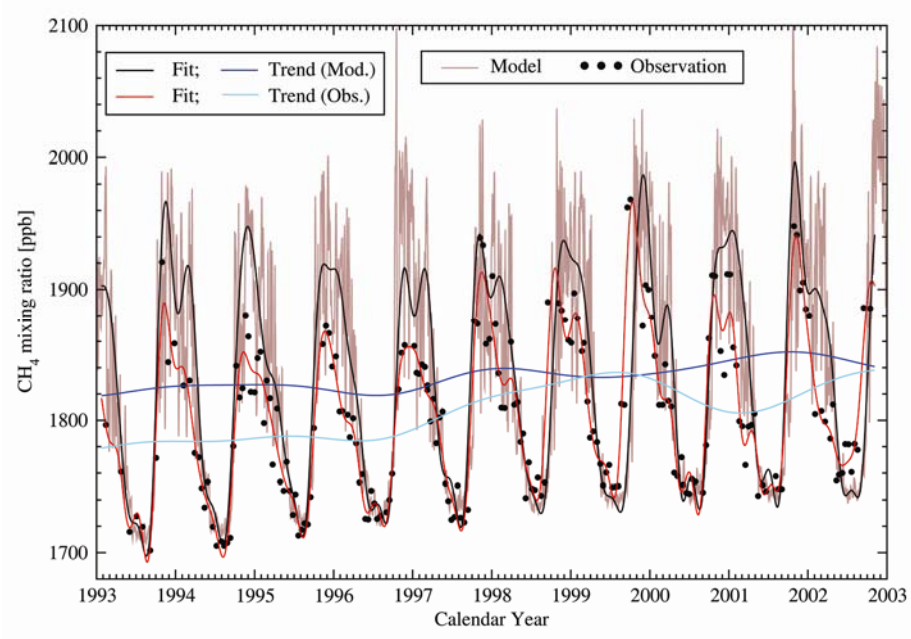

Figure 4. Model (brown line) and observation (black circle) comparison of CH_4 time series at CRI. The fitted curve (black and red lines) and long-term trend components (dark and light blue lines) as derived using a digital filtering technique are also shown for both observations and model results (see legends).

The ISV for CH_4 shows that high values persist only for the post SW-monsoon season when CH_4 emission from the Indian subcontinent is high, presumably due to rice cultivation, and then drop sharply during December–January indicating a rapid decline of the regional fluxes. These features are clearly captured by the ACTM model simulation, which is achieved by obtaining useful constraints on regional fluxes at different seasons of the year at this site as discussed in Patra *et al.*[20]. The IAV in CH_4 is in seemingly opposite phase to that for CO_2. During the El Niño periods the Indian subcontinent commonly receives below climatological average rainfall during the SW monsoon implying a lower area of inundation and agricultural activities[9]. Oceanic emissions of CH_4 at CRI can be ruled out since the Arabian Sea is not a significant source of CH_4, ranging from 0.0014 to 0.0024 g-CH_4 m^{-2} $month^{-1}$ over the period of the NE to SW monsoon seasons[31], compared to land fluxes in the range: 1–3 g-CH_4 m^{-2} $month^{-1}$.

The N_2O ISV peaks occur a couple of months earlier than that of CH_4 and are coincident with the SW monsoon season. Whether this is caused by the high oceanic emission during this season from the Arabian Sea as a whole[32] or more regionally from coastal upwelling[33] is a subject worth exploring in the future.

The CO IAV is somewhat similar to CO_2, again highlighting the role of fossil fuel and biomass burning related activities in mixing ratio IAVs around the CRI site for these two gases. Although CO ISVs looks closer to the CH_4 ISVs on the leading edge of the peak during autumn, the falling edge of this peak is delayed until late spring relative to that for CH_4. In fact, a secondary peak is systematically observed during spring in CO ISV.

Atmospheric trace gas studies at CRI were initiated by the Physical Research Laboratory, Ahmedabad and the National Institute of Oceanography, Goa, in collaboration with CSIRO Atmospheric Research, Aspendale, with the help and sponsorship of the International Atomic Energy Agency (IAEA). This set of measurements from Cabo de Rama, India provides important time series in a monsoonal zone of the Indian subcontinent for the first time. Enhanced levels of methane during NE monsoon period are thought to be due to various continental sources and, considering the agricultural practices in the Indian subcontinent, in particular the rice cultivation. To estimate the relative contribution of these sources, we have set up a methane extraction line at PRL to convert methane to carbon dioxide for isotopic analysis. These combined efforts are expected to be of great value in understanding the budget of the GHGs in earth's atmosphere. The CO seasonal variations are found to be similar to that for CH_4. The CO_2 time series has long been provided for inverse modelling studies of surface flux estimations through the GLOBALVIEW-CO_2 product[11] and its subsequent updates. The seasonal, inter-seasonal and inter-annual variations of CO_2 along with its $\delta^{13}C$–CO_2 and $\delta^{18}O$–CO_2 isotopic compositions help us to identify the governing mechanisms leading to the observed variations. Use of N_2O, CO and H_2 for inferring regional source/sink information appears promising based on the analysis of inter-seasonal and inter-annual variabilities. Noting the significance of this site in estimating the flux balance of

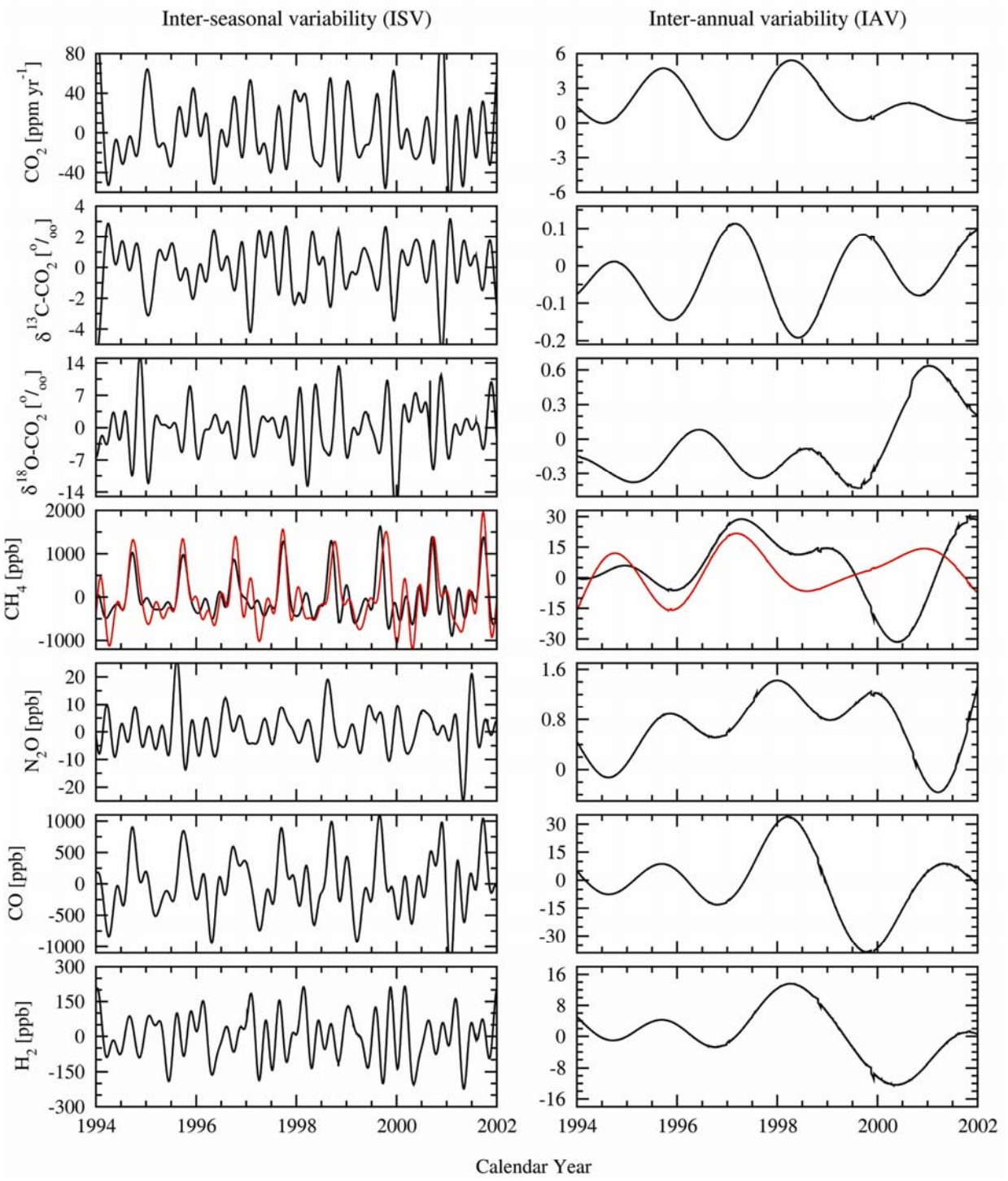

Figure 5. Comparisons of inter-seasonal and inter-annual variability in GHGs at CRI as obtained using the time derivatives of fitted curve and long-term trend (Figure 4) respectively. The ACTM results are shown for CH_4 only (red line).

the Indian subcontinent, we recommend that the observation programme at this site be continued and further sites be added for establishing a network of long-term monitoring of GHGs and their isotopic composition. More generally, in view of the persistent sea-breeze conditions for much of the year, high-resolution tracer transport modelling, supported by diurnal observations in representative wind regimes, would clarify and improve continental flux calculations.

1. Forster, P. *et al*., Changes in atmospheric constituents and in radiative forcing. In *Climate Change 2007: The Physical Science Basis. Fourth Assessment Report of the Intergovernmental Panel on Climate Change* (eds Solomon *et al*.), Cambridge University Press, Cambridge, UK, 2007, pp. 129–234.

2. Ehhalt, D. and Prather, M., Atmospheric chemistry and greenhouse gases, in climate change 2001: the scientific basis. Third Assessment Report of the Intergovernmental Panel on Climate Change (eds Houghton *et al.*), Cambridge University Press, Cambridge, UK, 2001, 239–287.
3. Rayner, P. J., Enting, I. G. and Trudinger, C. M., Optimizing the CO_2 observing network for constraining sources and sinks. *Tellus*, 1996, **48**, 433–444.
4. Patra, P. K. and Maksyutov, S., TransCom-3 modelers, sensitivity of optimal extension of CO_2 observation networks to model transport. *Tellus*, 2003, **55**, 498–511.
5. Lal, S., Chand, D., Venkataramani, S., Appu, K. S., Naja, M. and Patra, P. K., Trends in CH_4 and SF_6 at tropical site Thumba in India. *Atmos. Environ*., 2004, **38**, 145–151.
6. Sahu, L. K. and Lal, S., Distributions of C_2–C_5 NMHCs and related trace gases at a tropical urban site in India. *Atmos. Environ*., 2006, **40**, 880–891.
7. Rao, Y. P., South-west monsoon, Meteorol. Monograph, No. 1, India Meteorological Department, 1976.
8. Murty, C. S. and Murty, V. S. N., *The Indian Ocean: A Perspective* (eds Sengupta, R. and Desa, E.), Oxford & IBH, New Delhi, 2001, pp. 1–54.
9. Parthasarathy, B., Munot, A. A. and Kothawale, D. R., Regression model for estimation of Indian food grain production from Indian summer rainfall. *Agric. Forest Meteorol*., 1988, **42**, 167–182.
10. Francey, R. J. *et al.*, Global Atmospheric Sampling Laboratory (GASLAB): supporting and extending the Cape Grim trace gas programs. In *Baseline Atmospheric Program Australia* (eds Francey, R. J., Dick, A. L. and Derek, N.), Department of the Environment, Sport and Territories, Bureau of Meteorology in Cooperation with CSIRO Division of Atmospheric Research, Melbourne, 1996, pp. 8–29.
11. GLOBALVIEW-CO_2, Cooperative Atmospheric Data Integration Project – Carbon dioxide, CD-ROM, NOAA ESRL, Boulder, Colorado (Also available on Internet via anonymous FTP to ftp.cmdl.noaa.gov, Path: ccg/co2/GLOBALVIEW), 1996.
12. Rayner P. J., Law, R. M., Allison, C. E., Francey, R. J., Trudinger, C. M. and Pickett-Heaps, C., Interannual variability of the global carbon cycle (1992–2005) inferred by inversion of atmospheric CO_2 and $\delta^{13}CO_2$ measurements. *Global Biogeochem. Cycles*, 2008, **22**, GB3008.
13. Francey, R. J. *et al.*, Atmospheric carbon dioxide and its stable isotope ratios, methane, carbon monoxide, nitrous oxide and hydrogen from Shetland Isles. *Atmos. Environ*., 1998, **32**, 3331–3338.
14. Francey, R. J. *et al.*, The CSIRO (Australia) measurement of greenhouse gases in the global atmosphere. In Report of the 11th WMO/IAEA Meeting of Experts on Carbon Dioxide Concentration and Related Tracer Measurement Techniques, Tokyo, Japan, September 2001 (eds Toru, S. and Kazuto, S.), World Meteorological Organization Global Atmosphere Watch, 2003, pp. 97–111.
15. Allison, C. E. and Francey, R. J., Verifying southern hemisphere trends in atmospheric carbon dioxide stable isotopes. *J. Geophys. Res*., 2007, **112**, D21304.
16. Sturm, P. *et al.*, Permeation of atmospheric gases through polymer O-rings used in flasks for air sampling. *J. Geophys. Res*., 2004, **109**, D04309.
17. Cooper, L. N., Steele, L. P., Langenfelds, R. L., Spencer, D. A. and Lucarelli, M. P., Atmospheric methane, carbon dioxide, hydrogen, carbon monoxide, and nitrous oxide from Cape Grim flask air samples analysed by gas chromatography. In *Baseline Atmospheric Program* (*Australia*), *1996* (eds Gras, J., Tindale, N. and Derek, N.), Bureau of Meteorology and CSIRO Atmospheric Research, Melbourne, Australia, 1999, pp. 98–102.
18. Patra, P. K. *et al.*, Transport mechanisms for synoptic, seasonal and interannual SF6 variations and 'age' of air in troposphere. *Atmos. Chem. Phys*., 2009, **9**, 1209–1225.
19. Tiwari, Y. K. *et al.*, CO_2 observations at Cape Rama, India for the period of 1993–2002: Implications for constraining South Asian emissions using forward transport model simulations. *J. Geophys. Res*., 2009.
20. Patra, P. K. *et al*., Growth rate, seasonal, synoptic and diurnal variations in lower atmospheric methane. *J. Meteorol. Soc. Jpn*., 2009, **87**, 635–663.
21. Nakazawa, T., Ishizawa, M., Higuchi, K. and Trivett, N. B. A., Two curve fitting methods applied to CO_2 flask data. *Environmetrics*, 1997, **8**, 197–218.
22. Masarie, K. A. *et al.*, NOAA/CSIRO Flask Air Intercomparison Experiment: a strategy for directly assessing consistency among atmospheric measurements made by independent laboratories. *J. Geophys. Res*., 2001, **106**, 20445–20464.
23. Sarma, V. V. S. S., Kumar, M. D. and George, M. D., The eastern and central Arabian Sea as a perennial source for atmospheric carbon dioxide. *Tellus, Ser. B*, 1998, **50**, 179–184.
24. Patra, P. K., Ishizawa, M., Maksyutov, S., Nakazawa, T. and Inoue, G., Role of biomass burning and climate anomalies for land–atmosphere carbon fluxes based on inverse modelling of atmospheric CO_2. *Global Biogeochem. Cycles*, 2005, **19**, GB3005.
25. van der Werf, G. R. *et al.*, Climate regulation of fire emissions and deforestation in equatorial Asia. *Proc. Natl. Acad. Sci.*, 2008, **105**, 20350–20355.
26. Francey, R. J. and Tans, P. P., Latitudinal variation in oxygen-18 of atmospheric CO_2. *Nature*, 1987, **327**, 495–497.
27. Lelieveld, J. *et al.*, The Indian Ocean Experiment: widespread air pollution from South and South–East Asia. *Science*, 2001, **291**, 1031–1036.
28. Prinn, R. G., Cunnold, D. M., Rasmussen, R., Simmonds, P. G., Alyea, F. N., Crawford, A., Fraser, P. J. and Rosen, R., Atmospheric emissions and trends of nitrous oxide deduced from ten years of ALE-GAGE data. *J. Geophys. Res*., 1990, **95**, 18369–18385.
29. Huang, J. *et al.*, Estimation of regional emissions of nitrous oxide from 1997 to 2005 using multinetwork measurements, a chemical transport model, and an inverse method. *J. Geophys. Res.*, 2008, **113**, D17313.
30. Schmitt, S., Hanselmann, A., Wollschläger, U., Hammer, S. and Levin, I., Investigation of parameters controlling the soil sink of atmospheric molecular hydrogen. *Tellus B*, 2009, **61B**, 416–423.
31. Patra, P. K., Lal, S., Venkataramani, S., Gauns, M. and Sarma, V. V. S. S., Seasonal variability in distribution and fluxes of methane in the Arabian Sea. *J. Geophys. Res.*, 1998, **103**, 1167–1176.
32. Lal, S. and Patra, P. K., Variabilities in the fluxes and annual emissions of nitrous oxide from the Arabian Sea. *Global Biogeochem. Cycles*, 1998, **12**, 321–327.
33. Naqvi, S. W. A. *et al.*, Budgetary and biogeochemical implications of N_2O isotope signatures in the Arabian Sea. *Nature*, 1998, **394**, 462–464.

ACKNOWLEDGEMENTS. Several scientists and administrative personnel from CMAR (Aspendale), PRL (Ahmedabad) and NIO (Goa) contributed significantly towards the success of this programme. The trace gas measurements are crucially dependent on the sophisticated methods and equipment developed and maintained in CSIRO GASLAB. In this context, we are extremely thankful to Lisa Cooper, Darren Spencer, and Scott Coram. We are grateful to CSIRO Atmospheric Research for the scientific gift of the methane extraction line. Special thanks are due to the personnel at NOAA-ESRL, Boulder, Colorado, for providing the SEY data. We are also grateful for financial help received from the India–Australia Exchange Program and the Department of Science, Industry and Tourism, Australia, at various stages. We finally thank the Director of PRL, Chief of Division of CSIRO Atmospheric Research, and the Administrative Head at IAEA for encouragement and financial help to carry out this work. S.K.B. thanks Toshitaka Gamo for a Visiting Professorship to Ocean Research Institute, University of Tokyo during which the data analysis was completed.

Received 13 March 2009; revised accepted 15 September 2009